2,2-Dimethoxy-2-phenylacetophenone: Photochemistry and Free Radical Photofragmentation

Hanns Fischer,* Roger Baer, Roland Hany, Ingrid Verhoolen, and Manfred Walbiner
Physikalisch-Chemisches Institut der Universität Zürich, Winterthurerstrasse 190, CH-Zürich, Switzerland

Free radical reactions induced by photocleavage of the photocuring agent 2,2-dimethoxy-2-phenylacetophenone in oxygen-free solutions are investigated by product analysis, CIDNP, and by optical and ESR spectroscopy. It is shown that the photochemistry of the title compound is strongly influenced by both thermal and photochemical fragmentations of the α,α-dimethoxybenzyl radical. A resulting light intensity dependence of product distributions and spectra has caused previous misinterpretations of reaction mechanisms, reaction kinetics, and spectral assignments. Detailed mechanisms, optical spectra, and kinetic data on self-terminations, thermal fragmentations, and additions to acrylonitrile of dimethoxybenzyl, benzoyl, and related radicals are reported.

2,2-Dimethoxy-2-phenylacetophenone [DMPA, (**1**)] is an important photocuring agent (Irgacure 651, Ciba–Geigy) used mainly for acrylic and unsaturated polyester resins. Consequently, besides the technical applications, much work has been devoted to the unravelling of its photochemistry.[1–3] From product studies[4] and by analogy with related compounds[5,6] it seems clear that the primary reaction is a photochemical α-cleavage from a very short-lived triplet state ($\tau_T \leq 100$ ps) to α,α-dimethoxybenzyl (**R**^{1}) and benzoyl (**R**^{2}) radicals followed by a fragmentation of the dimethoxybenzyl radical to methyl benzoate and methyl (**R**^{3}). However, there are considerable discrepancies regarding the rate of demethylation and the relative efficiencies of the three radicals in initiating the radical polymerization. While a CIDNP study by Rist *et al.*[7] pointed to a fast demethylation in keeping with the observation of **R**^{2} and **R**^{3}, but not **R**^{1} by ESR,[8] Timpe *et al.*[9] report the trapping of **R**^{1} and **R**^{2}, but not **R**^{3}, by *N*-t-butyl-α-phenylnitrone, which indicates slow fragmentation. In a more recent time-resolved ESR experiment[10] all three radicals were observed 0.3 μs after laser pulses which again was ascribed to a fast reaction while an early steady-state investigation in these laboratories[11] employing radical lifetimes of 500 μs revealed the presence of **R**^{1} and **R**^{2} at room temperature. Very minute signals of **R**^{3} appeared only at 70 °C. Moreover, Hagemann *et al.*[8] showed that **R**^{2} and **R**^{3} add to 1,1-diphenylethene, while **R**^{1} is only involved in terminations. This contrasts somewhat with Timpe's findings,[9] and the statement of Fouassier *et al.*[6,12] that **R**^{1} is at least as efficient as **R**^{2} in initiating the polymerization of methyl methacrylate. Finally, Fouassier *et al.*[6] determined optical absorptions of transients after flash photolysis of DMPA, though only for $\lambda \geq 380$ nm. The spectrum attributed to **R**^{2} only very vaguely resembles the known spectrum of benzoyl[13] and that attributed to **R**^{1} has no similarity to authentic spectra of other α-oxy-substituted benzyls.[14,15] Also, Fouassier's spectra do not match those of other authors.[16] Recently, we have shown[17] by a fast time-resolved ESR technique that the dimethoxybenzyl radical **R**^{1} formed by photolysis of DMPA undergoes, with a sufficient light intensity at 308 nm, a facile photofragmentation to methylbenzoate and methyl. Such a process is paralleled for α-oxy substituted benzyls,[18] and it means that product distributions, CIDNP effects, optical and ESR spectra and the importance of **R**^{1} *vs.* **R**^{3} in polymerizations with DMPA will depend on the intensity of photolysis. Even all CH_3-radicals may have been formed by photo- and not thermal fragmentation of **R**^{1}. In view of our long-standing interest in the system,[11] we have now restudied the photochemical behaviour of DMPA by a variety of techniques and for various light intensities. We show that the conclusions of much of the previous work are obsolete now because the photofragmentation reaction was not considered.

Experimental

All chemicals were used in the purest forms available from commercial sources or from Ciba–Geigy. Solutions were freed from oxygen prior to use either by freeze–pump–thaw cycles (for CIDNP and product analysis using pulsed laser photolysis) or by purging with noble gases (for ESR and optical spectroscopy).

Product analyses were performed by GLC using authentic compounds for identification and calibration. For this purpose methyl *o*- and *p*-benzoylbenzoate, and the dimethylacetals of acetophenone and of *p*-benzoylmethylbenzoate were synthes-

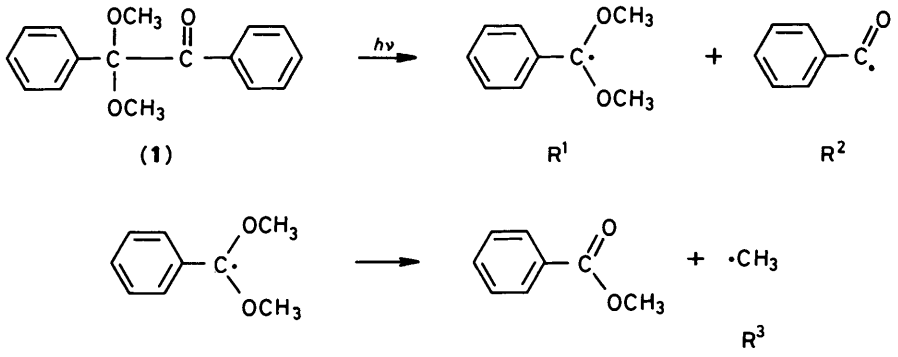

ized by conventional routes, since they were not available commercially. The α,α-dimer of $\mathbf{R^1}$, *i.e.* 1,2-diphenyl-1,1,2,2-tetramethoxyethane has not been described previously and was prepared photochemically as follows. A solution consisting of t-butyl alcohol (17 g), acetonitrile (10 g), α,α-dimethoxytoluene (12 g), and di(t-butyl) peroxide (61 g) was photolysed at 10–13 °C under N_2-flushing in a photochemical reactor (Mangels) with a 125 W Philips HPK lamp for 3 h, to about 80% conversion of the toluene. The crude reaction mixture showed a 10% yield of the desired product formed *via* Scheme 1. Work-up

$$(CH_3)_3COOC(CH_3)_3 \xrightarrow{h\nu} 2(CH_3)_3CO^{\bullet}$$

$$(CH_3)_3CO^{\bullet} + PhCH(OCH_3)_2 \longrightarrow (CH_3)_3COH + Ph\dot{C}(OCH_3)_2$$

$$\mathbf{R^1}$$

$$2\mathbf{R^1} \longrightarrow PhC(OCH_3)_2C(OCH_3)_2Ph$$

Scheme 1.

revealed the product as a crystalline solid (m.p. 52 °C). CIDNP spectra of reaction products free from thermal equilibrium signals were obtained 2 μs after 308 nm laser pulses, under conditions of low conversion (D = 0.87, conversion 2–10%, total absorbed energy at maximum 30 mJ/pulse). The technical details for sample preparation, data analysis and the procedures for the calculation of CIDNP intensities followed previous descriptions.[19,20]

The optical spectra of transients and their kinetics were obtained under modulated excitation with the apparatus described earlier in detail,[21] which had been modified to allow digital data storing and handling. In comparison with flash photolysis[6] this method has the advantage of recording spectra of transients within the near-UV transitions of DMPA, *i.e.* for 300 nm $\leq \lambda \leq$ 390 nm also, and not only above this region. The photolysis light was filtered to the 360 nm region using as previously described.[21] Conversion levels were kept below 15%.

Finally, the ESR spectra were taken also at low conversion levels in a flow apparatus.[22]

Results and Discussion

Product Studies.—Sandner and Osborn[4] reported photolysis products of DMPA in a variety of solvents, presumably for fairly high conversion and without exclusion of oxygen. They found methyl benzoate in 45–61% yield, benzaldehyde (17–20%), benzil (7–11%), and acetophenone (2–8%). While these products are in accord with the above mentioned reactions, the material balance was poor, and the formation of benzaldehyde is obscure since benzoyl radicals are not likely to abstract hydrogen atoms from the solvents, *e.g.* benzene. Davidson *et al.*[23] reported the products of decomposition of DMPA in dinonyl phthalate on paper, in a curing apparatus for 100% conversion under aerobic conditions. Besides methyl benzoate they found methyl anisolate, methyl *o*- and *p*-benzoylbenzoate and benzoic acid as major components, and benzaldehyde, benzophenone, benzil, acetophenone, and biphenyl in minute amounts. Product balances were not given. Some of the products mentioned were also observed by Phan.[24]

In his important CIDNP investigation Rist[7] employing high intensity CW photolysis of oxygen-containing solutions proved a number of mechanistical details, *i.e.* reformation of DMPA by coupling of $\mathbf{R^1}$ and $\mathbf{R^2}$ at the α-positions accompanied by the formation of *o*- and *p*-semibenzenes by coupling of $\mathbf{R^2}$ at the *ortho* and *para* positions of $\mathbf{R^1}$, formation of methyl benzoate by demethylation of $\mathbf{R^1}$ and the coupling of $\mathbf{R^2}$ and $\mathbf{R^3}$ to give acetophenone. Several CIDNP signals were not identified; benzaldehyde showed a remarkable phase inversion with time, but the primary cleavage clearly resulted from triplet DMPA. Further, he reports the detection of methyl-substituted methyl benzoates by GC–MS. The formation of semibenzenes in cross-terminations of benzyl with other radicals is well known.[25] Under conditions of high radical concentrations they are likely to serve as hydrogen atom donors,[7] and the resulting substituted radicals of type $\mathbf{R^2}$ are likely precursors for the benzoyl-and the methyl-substituted methyl benzoates observed.[7,23]

Scheme 2 shows the major radical reactions which we envisage on the basis of the previous findings and usual radical chemistry. It also gives the abbreviations for the various products used below. For the semibenzenes (**2**), (**5**), and (**9**) and their products (**11**), (**12**), and (**13**) only the *para*-addition structures are drawn. Reactions of radicals with our solvents (**14**), acetonitrile, benzene, and cyclohexane, are unlikely for $\mathbf{R^1}$ and $\mathbf{R^2}$, because they are rather endothermic. If the scheme is complete and if the semibenzenes are intermediates only, the yields of products containing group $\mathbf{R^1}$ or its methyl benzoate residue should balance the yields of products containing $\mathbf{R^2}$ as: [(**3**)] + 2{[(**4**)]} + [(**8**)] + 2{[(**11**)]} + [(**12**)] + [(**13**)] + [(**16**)] = 2{[(**6**)]} + [(**7**)] + [(**12**)] + [(**14**)], and these sums should also equal the DMPA consumption. For large conversions the balance can easily be off-set by photoreactions of products absorbing in the same region as DMPA, namely (**6**), (**7**), (**11**), and (**14**). In the earlier studies[4,23] the yields of these products were low, undoubtedly due to such secondary photoreactions.

The fraction of demethylation P_{DEM} of the dimethoxybenzyl radical $\mathbf{R^1}$ [reaction (3)] is given by the ratio of the yield of methyl benzoate (**3**) to the total yield of $\mathbf{R^1}$ groups in the products. In the following we will assume that the fragmentation occurs both *via* photochemical and thermal pathways. Since $\mathbf{R^1}$ absorbs in the same region as DMPA (see optical spectra below), we expect that for high photolysis rates, *i.e.* conditions of high radical concentrations, P_{DEM} approaches unity because of complete photodemethylation. If the thermal demethylation is not too fast to overrule the $\mathbf{R^1}$ terminations P_{DEM} should then decrease with decreasing photolysis rate. For very low light intensities it should increase again, because eventually the termination reactions will become slow enough to allow complete thermal demethylation. To test this hypothesis we have performed two sets of experiments under entirely different photolysis conditions. In the first set, samples were taken after low-intensity modulated CW irradiation of 2.2×10^{-3} mol dm^{-3} solutions of DMPA in acetonitrile at room temperature after passing the cell of the optical modulation spectroscopy apparatus. In one run (run 1) the conditions used for the recording of the optical spectra were applied, in the second (run 2) those used for obtaining kinetic data (see below). The second set of experiments involved exposure of 50 mm^3 samples (3×10^{-3} mol dm^{-3} DMPA in acetonitrile, in sealed degassed ampoules) to the focussed 308 nm radiation of a pulsed Lambda Physics excimer laser (LPX 100) with nominal absorbed energy of 100 mJ/pulse. By filtering with aqueous $KCr(SO_4)_2$ solutions and insertion of filter glasses and glass plates of known transmissions, the incident intensity was varied over more than four orders of magnitude, and the number of pulses applied to the samples was adjusted so that the total accumulated photolysis energy was kept constant.

Table 1 shows the products observed for the low intensity CW photolysis and their distribution (average of 3 samples each). The major components are methyl benzoate, benzil, methane, and the methyl benzoylbenzoates from the cross-termination of $\mathbf{R^1}$ and $\mathbf{R^2}$ (*para*:*ortho* = 3:1). The dimers of $\mathbf{R^1}$ *i.e.* (4) and (12), and acetophenone and benzaldehyde contribute to lower extents. The balance of $\mathbf{R^1}$– and $\mathbf{R^2}$– groups is excellent, which excludes secondary photoreactions of the products.

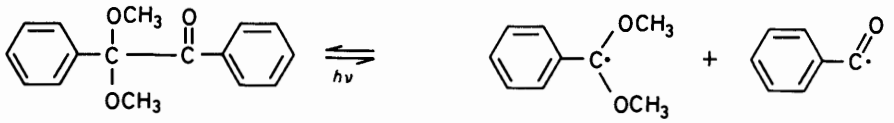

(1) (1)

R1 R2

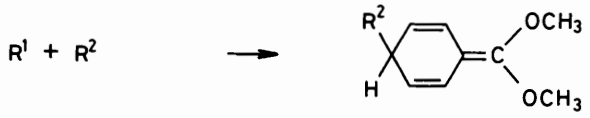

(2)

(2*p*) [+(2*o*)]

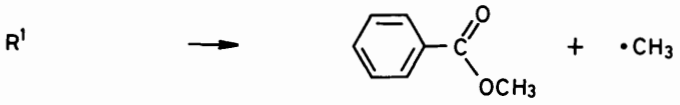

(3)

(3) R3

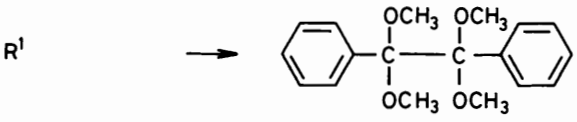

(4)

(4)

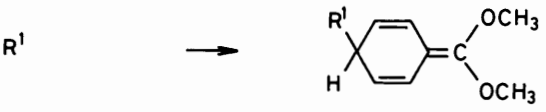

(5)

(5*p*) [+(5*o*)]

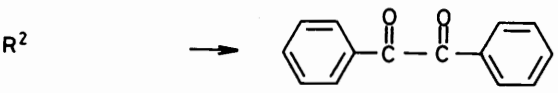

(6)

(6)

(7)

(7)

(8)

(8)

(9)

(9*p*) [+(9*o*)]

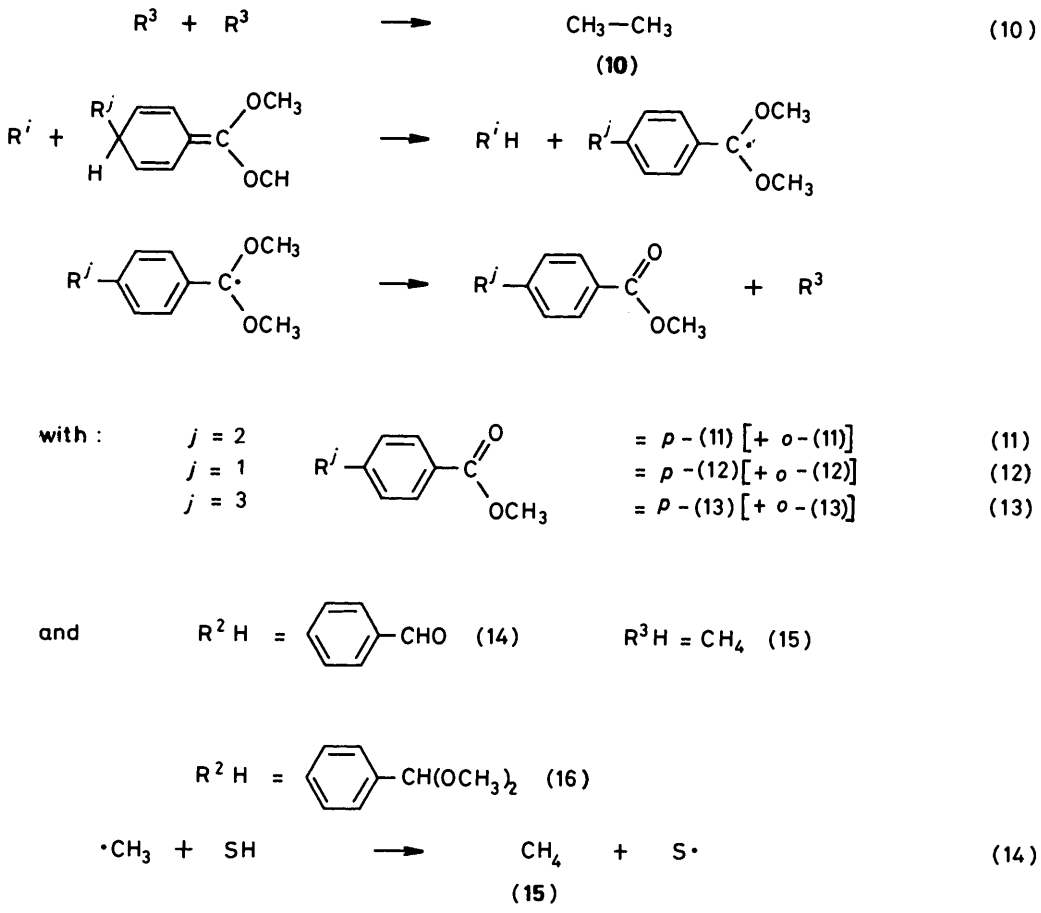

Scheme 2. Reactions after photocleavage of 2,2-dimethoxy-2-phenyl acetophenone.

Table 1. Products of low-intensity CW-photolysis.

		Run 1[a]		Run 2[b]	
Product	Radicals	Conc./μmol dm^{-3}	%(R^1)[(R^2)]	Conc./μmol dm^{-3}	%(R^1)[(R^2)]
(3)	R^1	73	56	114	55
(4)	2R^1	6.5	10	13	13
(6)	2R^2	39	[66]	67	[67]
(7)	R^2 + R^3	5	[4]	9	[5]
(8)	R^1 + R^3	5	4	9	4
o-(11) + *p*-(11)	R^1 + R^2	8 + 24	24, [27]	9 + 42	25, [25]
o-(12) + *p*-(12)	2R^1	0 + 4	6	4	4
(14)	R^2	4	[3]	7	[4]
(15)	R^3	90	—	130	—
Total	ΣR^1	131		208	
products	ΣR^2	119		201	

[a] Conditions as for Figure 8, DMPA conversion 8%, (80 ± 7)% identified as products. [b] Conditions as for Figure 10, DMPA conversion 14%, (70 ± 7)% identified as products.

Benzoic acid, methyl anisate, benzophenone, and biphenyl which had been reported earlier[23] were not found, nor were methyl-substituted methyl benzoates[7] and ethane. The formation of benzoic acid and an increased yield of benzaldehyde was observed in incompletely deoxygenated samples, however. The probability of demethylation is about 0.55 and slightly larger in the sample irradiated with lower intensity (run 1). This suggests a dominant thermal fragmentation. Of the methyl radicals formed together with (3), (11), and (12), only a minor fraction [(7), (8)] reacts by cross-termination with R^1 and R^2. The major part abstracts a hydrogen atom from acetonitrile and forms methane and $^{\bullet}CH_2CN$. The fate of the latter radical could not be established, but by reactions with R^1, R^2, and R^3 and with the semibenzenes it will give rise to a large variety of products. In fact, quite a number of small additional components were detected besides those listed in Table 1 but could not be identified. In part they are responsible for the fact that 20–30% of the decomposed DMPA did not appear as products. On the other hand, the large yields of methane and the absence of ethane are in accord with a fairly long lifetime of the

Table 2. R^1-products of pulse laser photolysis at various light intensities.

I_0	N	Product (3)	(4)	(8)	*o*-(11) + *p*-(11)
1[b]	1	97[a]	1.4	1.4	—
4.8×10^{-1}	2	96	1.5	2.2	—
1.2×10^{-1}	8	80	2.0	5.6	12.4
2.1×10^{-2}	48	70	7.3	7.3	15.4
7.6×10^{-3}	131	67	18	9.2	5.4
1.9×10^{-3}	512	46	33	5.5	15.2
5.0×10^{-4}	2 000	58	22	6.4	13.4
6.6×10^{-5}	1.5×10^4	82	9	4.0	8.4

[a] Percentage values. [b] Relative values. [c] Number of irradiations.

total radical population and point to rather slow thermal demethylation of R^1.

Table 2 gives the essential results of the pulse laser photolysis for various pulse intensities. For these runs conversions were between 10 and 25%, and the ratio of R^1 to R^2 groups reappearing in the products scattered between 1.2 and 2, which indicates secondary photoreactions of R^2 products. As expected above, for high intensity irradiation methyl benzoate is virtually the only product of R^1. This indicates nearly quantitative photofragmentation. With decreasing irradiation intensity its yield decreases and then increases again as the thermal reaction competes with termination. The other R^1 products show the opposite behaviour. In addition, the composition of gaseous products was found to vary from pure ethane at high intensities to pure methane at low intensities. This is also as expected since for lower light intensities, *i.e.* lower initial radical concentrations, reaction (14) will compete more effectively with the termination reaction (10).

In Figure 1 the fraction of demethylation of R^1 is plotted *vs.* the logarithm of relative pulse energy. Also shown (solid curves) are calculated dependencies for pure photofragmentation (left) and pure thermal fragmentation (right). For the former, reactions (1) and (3) create and deplete R^1 during the pulse (τ_p *ca.* 20 ns) and lead to equation (15) where c is a constant

$$P_{DEM} = 1 - \frac{1}{c\tau_p I}[1 - \exp(-c\tau_p I)] \qquad (15)$$

containing the photophysical properties of R^1. It was adjusted to match the calculated curve to the experimental points at the high intensity branch. To obtain the curve for thermal fragmentation (right) we set the self-termination rate constants $2k_{ii}$ of all radicals equal to a common $2k_t$ and set all cross-termination constants equal to this, $k_{ij} = 2k_t$. This approximation will be justified later on. It leads to the kinetic equations (16) and (17), when [R] is the total radical concentration

$$[R^1] = -\{k_3 + 2k_t[(R)]\} \times [R^1] \qquad (16)$$

$$[\dot{3}] = k_3[R^1] \qquad (17)$$

$[R]_t = [R]_0(1 + t/\tau_t)^{-1}$ with the termination lifetime $\tau_t = (2k_t[R]_0)^{-1}$. Equations (16) and (17) were integrated numerically for various values of $k_3\tau_t$, and the scale was adjusted so that the curve matched the data on the low intensity side of Figure 1. Evidently, the regions of dominant photochemical and thermal fragmentation overlap to some extent. The large experimental errors and the unknown absolute pulse energy absorbed do not allow more than this qualitative analysis, but it clearly demonstrates that both pathways occur and that their relative contributions vary with the experimental conditions.

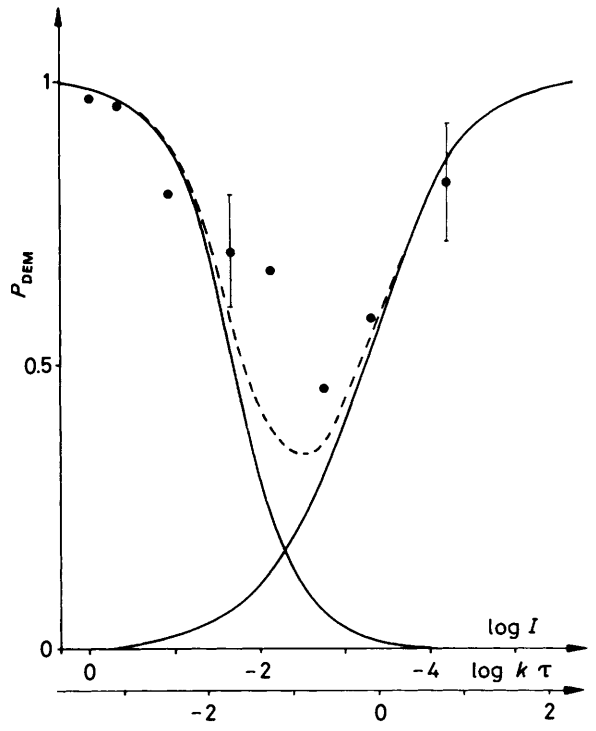

Figure 1. Fraction of demethylation of the α,α-dimethoxybenzyl radical *vs.* photolysis intensity. For calculated curves, see the text.

Chemically Induced Dynamic Nuclear Polarization.—200 MHz proton CIDNP spectra (net effects only) of the radical reaction products of DMPA photolysis in ($^2H_3$)acetonitrile and ($^2H_{12}$)cyclohexane were taken 2 μs after application of 20 ns pulses (308 nm) of a Lambda Physics excimer laser EMG 100. The solutions were 1.7×10^{-2} mol dm^{-3} in DMPA, and the optical arrangement delivered about 30 mJ/pulse to the sample for the maximum laser output of 120 mJ/pulse directed to the probehead. A presaturation pulse was applied to avoid contributions of thermal equilibrium signals, as before.[19,20] To obtain sufficient signal-to-noise ratios, FIDs of several irradiations were accumulated. The overall conversions of DMPA were kept below 10%, and in experiments using different incident pulse energies (adjusted by insertion of glass plates in the laser beam) the number of irradiations was adjusted to keep the total energy constant.

Figure 2(*a*) shows a CIDNP spectrum obtained for ($^2H_{12}$)-cyclohexane solutions at the highest available light intensity. Very similar spectra were observed for ($^2H_3$)acetonitrile solvent with the exception of the line at δ 9.64 which was missing. The spectra showed only a minor time dependence in the μs-region which means that the overall radical lifetime is of this order of magnitude, and that the CIDNP effects are due to both geminate and non-geminate (F-pair) radical reactions occurring on that timescale. The assignments of the CIDNP peaks to various products are noted in Figure 2 and are repeated in Table 3 together with additional information. A comparison with the 100 MHz spectrum obtained by Rist[7] in ($^2H_6$)benzene for CW photolysis shows good agreement, in general. New features are the identifications of (**4**), (**8**), and *o*,*p*-(**9**) and the observation of polarizations of the CH_3 groups of (**1**) and (**3**). Also, we find the formation of ethane (**10**) and not methane. The signal at δ 9.64 is definitely not benzaldehyde nor a methylated derivative. It was not observed for acetonitrile solvent, and its origin remains obscure.

Table 3. Assignments of CIDNP effects.

Product	Protons	δ(ppm)[a]	CIDNP[b]
(1)	$-OCH_3$	3.19	A
	$-H_o$ (benzyl)	7.62	E
	$-H_{m,p}$ (benzyl)	*ca.* 7.2	A,E
p-(2)	$-OCH_3$	3.59	A
	$-H_p$ (semibenzene)	4.74	E
	$-H_o$ (semibenzene)	6.46	E
	$-H_m$ (semibenzene)	5.60	A
o-(2)	$-OCH_3$	3.49	A
	$-H_{o,p}$ (semibenzene)	5.87, 6.36	E
(3)	$-OCH_3$	3.84	E
	$-H_o$	8.04	A
	$-H_p$	7.43	A
(4)	$-OCH_3$	3.62	E
(7)	$-CH_3$	2.48	E
(8)	$-CH_3$	1.49	A
o-,*p*-(9)	$-CH_3$	1.05, 1.09	A
(10)	$-CH_3$	0.90	A

[a] Referenced to TMS. [b] A = enhanced absorption, E = emission.

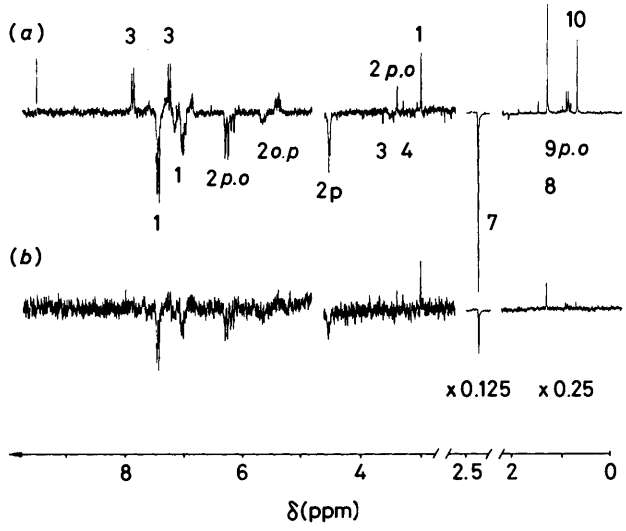

Figure 2. Net proton CIDNP effects after pulse photolysis of DMPA: (*a*) 117 mJ/pulse delivered to the NMR probehead, 17 scans averaged; (*b*) 27 mJ/pulse delivered, 75 scans. For assignments, see the text.

With the aid of Kaptein's rules[26] and the known magnetic properties of the radicals[10,27] ($\mathbf{R}^1$: g = 2.0028, $2H_o$: −0.496 mT, $2H_m$: +0.162 mT, H_p: −0.599 mT, $6CH_3$: +0.027 mT; $\mathbf{R}^2$: g = 2.0006, $2H_o$: +0.021 mT, $2H_m$: +0.021 mT, $2H_m$: +0.118 mT, H_p: +0.007 mT; $\mathbf{R}^3$: g = 2.0025, 3H: −2.28 mT) the signs of the net CIDNP effects are easily explained in terms of the reactions of Scheme 2, *i.e.* (1) and (2) are formed from geminate triplet pairs after α-cleavage and from non-geminate pairs ($\overline{\mathbf{R}^1\mathbf{R}^2}$) [equations (1) and (2)]. (3) and (4) are escape products of these pairs. The polarization of (7) arises in reaction (7) and that of (8) in reaction (8), *i.e.* from non-geminate (F) pairs. The enhanced absorption of ethane is due to escape from (7).

It should be noted that the magnitudes of the CIDNP effects do not directly correspond to the relative importance of the various pair reactions. Table 4 shows absolute net nuclear polarizations per radical pair calculated with the refined re-

Table 4. Calculated absolute net nuclear polarizations per radical pair.

Product	Group	$(P/\Delta M) \times 10^4$
(1)[a]	OCH_3	+3.1
	H_o (benzyl)	−19.0
	H_m (benzyl)	+6.2
	H_p (benzyl)	−11.5
(7)[b]	CH_3	−65.5
	H_m	−2.3
(8)[b]	CH_3	+34.1
	OCH_3	−0.2
	H_o	+1.0
	H_m	−1.3
	H_p	+1.3

[a] Geminate T-pair. [b] F-pair.

encounter model of ref. 20. Relative diffusion coefficients of the radicals and reaction distances were estimated by usual procedures and small-step diffusion was assumed.[20,22] Obviously, the pairs $\overline{\mathbf{R}^1\mathbf{R}^3}$ and $\overline{\mathbf{R}^2\mathbf{R}^3}$ of reactions (7) and (8) create considerably larger polarizations than the primary geminate pairs $\overline{\mathbf{R}^1\mathbf{R}^2}$. Thus, little can be said about the fraction of demethylation from the sizes of CIDNP effects directly. However, from relative polarizations an additional mechanistic detail is deduced. The ratio of polarizations of (1) and *p*-(2) is 2.2 ± 0.1 and that of *p*-(2) and *o*-(2) 2.5 ± 0.2, so that the ratio of combination of the pair $\overline{\mathbf{R}^1\mathbf{R}^2}$ to DMPA and to the semibenzenes (2) is 1.6 ± 0.1. It is comparable to the value found in benzene[7] and much lower than the ratio (= 5) for pairs of unsubstituted benzyl radicals,[24] probably because of steric hindrance.

The observation of 'escape-type' polarization of methyl benzoate has been taken as evidence[7] for a fast thermal fragmentation of the dimethoxybenzyl radical, since it would be strongly diminished by nuclear relaxation if it occurred in times longer than about 100 μs, *i.e.* the typical nuclear relaxation time[19] of radicals. However, the following findings prove that the fragmentation occurs photochemically under our conditions. The lower part of Figure 2 shows a CIDNP spectrum obtained with a lower pulse energy. In relation to the intensity of the pair products (1) and (2), those of the ester (3) and of the $\mathbf{R}^3$-derived products (7), (8), and (10) appear drastically reduced. Since a reduced pulse energy corresponds to a prolonged overall radical lifetime just the opposite behaviour would have been observed if the fragmentation were thermal.

Figures 3 and 4 quantify the intensity dependences. They show polarizations per radical pair for several products *vs.* the pulse energy. There is no dependence for the pair products (1) and (2). The ester (3) and products containing one methyl radical *i.e.* (7) and (8) show a linear increase, and ethane (10), composed of two methyl radicals, shows a quadratic increase. The interpretation is as follows: during the laser pulse of about 20 ns, radical pairs $\overline{\mathbf{R}^1\mathbf{R}^2}$ are created and react to produce the polarized products (1) and (2) on the 100 ps to 10 ns timescale typical for CIDNP formation in low viscosity solvents.[28] Their polarization is proportional to the concentration of pairs ΔM. This increases linearly with the pulse energy, *i.e.* $P/\Delta M$ does not depend on this quantity. The escaping dimethoxybenzyl radicals absorb within the same pulse and fragment thereafter. The probability of this process is proportional to ΔM *and* the pulse energy (for low radical absorbance) *i.e.* $P/\Delta M$ becomes proportional to the intensity for the corresponding products (3), (7), and (8). The formation of ethane requires two CH_3 radicals which explains the quadratic dependence. These findings also point to a short life-time of excited DMPA (not exceeding several nanoseconds) and of the excited dimethoxybenzyl radical.

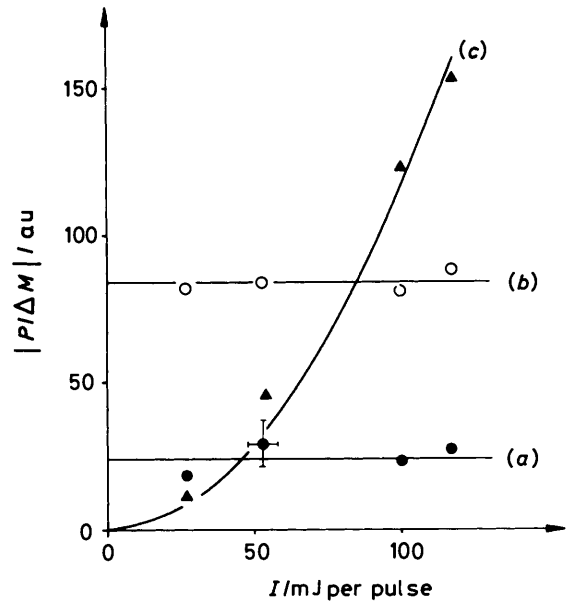

Figure 3. Net nuclear polarizations of reaction products *vs.* pulse energies delivered to the probehead: (*a*) DMPA (**1**) (OCH_3); (*b*) *p*-semibenzene *p*-(**2**) (H_o); (*c*) ethane (**10**).

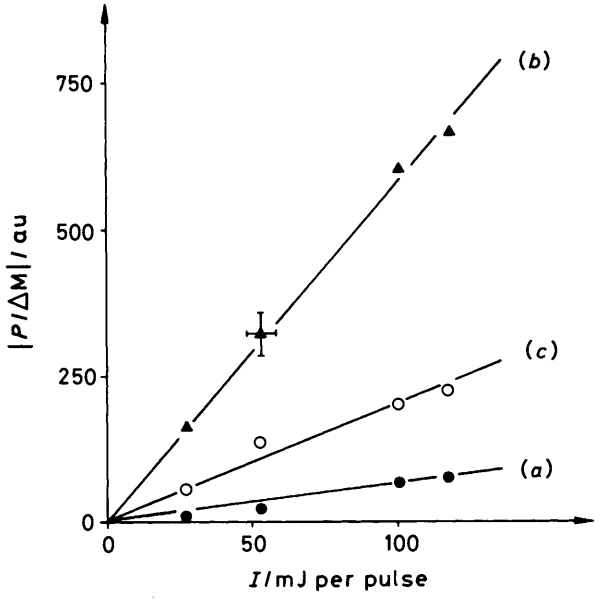

Figure 4. Net nuclear polarizations of reaction products *vs.* pulse energies delivered to the probehead: (*a*) methyl benzoate (**3**) (H_o); (*b*) acetophenone (**7**) (CH_3); (*c*) 1,1-dimethoxy-1-phenylethane (**8**) (CH_3).

The 'spin-sorting' character of CIDNP[28] also allows a direct determination of the fraction of photochemical demethylation from the ratio of the polarizations of (**3**) and of the pair products (**1**) and (**2**). It was found to increase from 5 to 25% with pulse energies varying from 27 to 117 mJ. Finally, the observations indicate that non-geminate reactions contribute only marginally to the polarizations of (**1**), (**2**), and (**3**), presumably due to effective cancellation.[19]

A clear indication of the photofragmentation is already contained in Rist's previous CIDNP work.[7] He reported that addition of methyl acrylate in 0.1–0.2 mol dm^{-3} concentrations completely quenched the polarization of acetophenone (**7**) whereas that of (**3**) was only reduced by about 50% and then remained constant up to 0.8 mol dm^{-3}. The quenching of (**7**) and

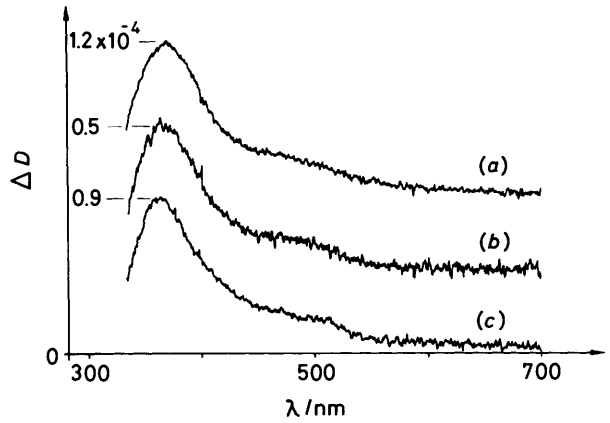

Figure 5. Optical spectra (ν = 77 s^{-1}, T = 26 °C) of benzoyl obtained from photolysis of various aryl ketones. For the structures of (*a*), (*b*), (*c*) see the text.

the partial reductions of (**3**) are, of course, caused by addition of R^2 and R^3 to the alkene which prevents the formation of non-geminate pairs. The remaining fraction of (**3**) is now explained by the photofragmentation process. We repeated the quenching experiment with methyl methacrylate as the alkene. Again all non-geminate polarizations were quenched at low concentrations. (**1**), (**2**), and (**3**) showed Stern–Volmer type quenching behaviour with $k_q \times \tau = 0.15$, *i.e.* considerable quenching only above concentrations of 1 mol dm^{-3}. Addition of the benzoyl radical of the primary pair is unlikely to be the cause since the rate constant is expected to be similar to that of related acyl radicals (*ca.* 5×10^5 dm^3 mol^{-1} s^{-1} at 300 K[29]) which leads to an unacceptably long pair life-time; also unlikely is addition of the dimethoxybenzyl radical (see below). A near-diffusion-controlled quenching of the DMPA triplet appears more attractive and would confirm the short triplet life-time in the 100 ps to 1 ns region stated above and before.[5,12]

Optical Spectroscopy and Reaction Kinetics.—Optical Spectra of the Radicals. The ketone and diketone products of DMPA photolysis (Scheme 2) absorb in the same wavelength region as DMPA, may have long-lived triplet states and lead to secondary arylketyl radicals by photoreduction, which also absorb in this region. Furthermore, both radicals of interest here, *i.e.* benzoyl and α,α-dimethoxybenzyl are expected to absorb in the blue and near UV region.[13–15] This makes the observation of the primary transients of DMPA photolysis by optical spectroscopy particularly difficult. The spectra may easily be contaminated by contributions of other species. The photofragmentation of dimethoxybenzyl adds to the difficulties since it may also be caused by the analysing light beam. Therefore, the following studies were carried out with low intensity photolysis of DMPA restricted to the 365 nm region,[13] low analysing power, and for low conversions. Moreover, benzoyl, and dimethoxybenzyl were generated also from other sources besides DMPA. Acetonitrile was used as solvent since it is a poor photoreducing agent.

Figure 5 shows optical spectra of transients observed during modulated photolysis of three ketones (*a*), (*b*), and (*c*), which from ESR identifications are known to yield benzoyl and alkyl radicals upon photocleavage. The α-oxysubstituted alkyls do not absorb markedly above λ *ca.* 300 nm,[30,31] *i.e.* the absorptions are expected to arise from benzoyl radicals only. In fact, they agree very well with a previous spectrum of benzoyl obtained from photolysis of pivalophenone.[3]

In all systems involving benzoyl radicals one major spectral contamination can be the photoreduction product

Table 5. Optical properties and self-termination rate constants of radicals at 25 °C.

Radical	λ_{max}/nm	ε/dm^3 mol^{-1} s^{-1}	$2k_t/10^9$ dm^3 mol^{-1} s^{-1}	Ref.
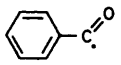	370	*ca.* 150	1.3[b] 2.6	13 This work
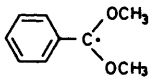	304[a] 318[a] 418	6 300 4 200 800	2.6	This work
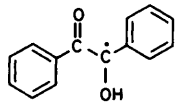	370 495[a]	8 800 2 000	1.1[c]	15

[a] Pronounced shoulder. [b] In 3-methylpentan-3-ol. [c] In water.

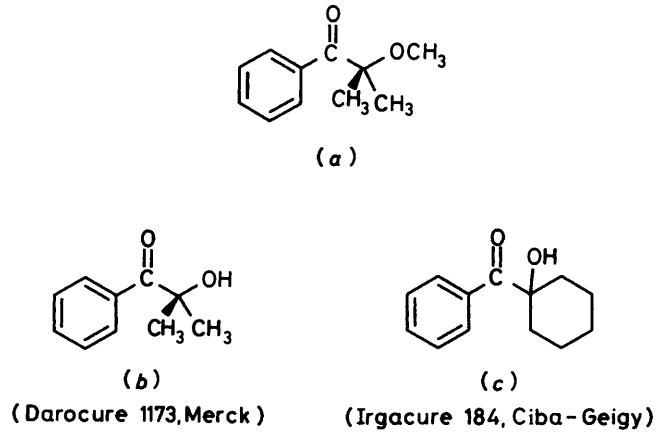

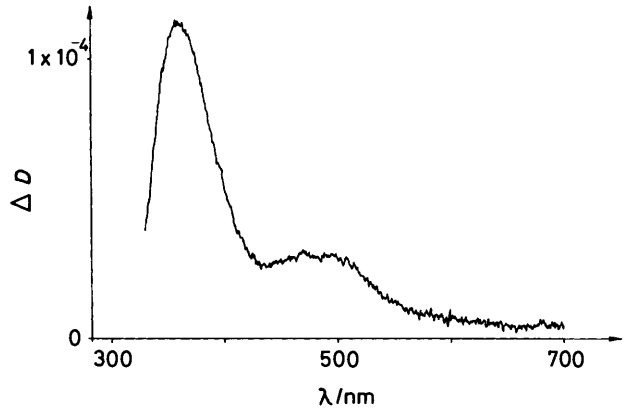

Figure 6. Optical spectrum (ν = 78 s^{-1}, T = 25 °C) of PhCOĊOHPh in acetonitrile–propan-2-ol mixture.

PhCOĊOHPh of benzil, the result of the benzoyl self-termination. Figure 6 shows the spectrum of this radical obtained during photolysis of 1.2 × 10^{-3} mol dm^{-3} benzil in acetonitrile–propan-2-ol (4:1 by volume) mixtures. It is very similar to that of benzoyl (Figure 5) with the major differences being a clear minimum between the maxima at 370 and 495 nm and completely different molar absorption coefficients (Table 5), leading to higher absorbances. In pure acetonitrile PhCOĊOHPh could not be observed. The striking similarity of the spectra of benzoyl and the benzil ketyl radical has lead to misinterpretations; based on the similarity of the spectra

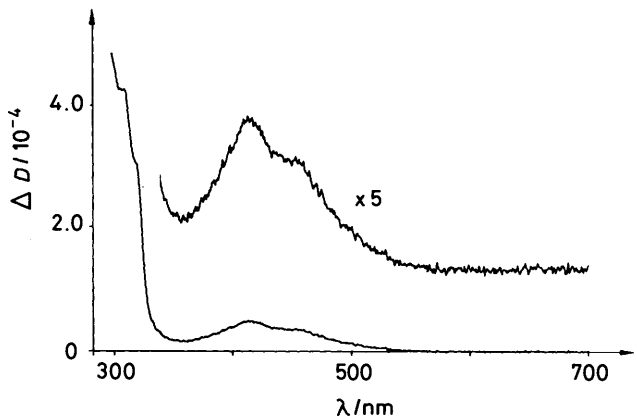

Figure 7. Optical spectrum (ν = 77 s^{-1}, T = 25 °C) of PhĊ(OCH$_3$)$_2$ derived from PhCH(OCH$_3$)$_2$ in acetonitrile.

obtained after photolysis of benzil and the ketones (*b*) and (*c*) and their assignment to benzoyl Allen *et al.* recently concluded that benzil is clearly a photofragmenting-type polymerization initiator.[16] This statement is completely at variance with the well established photochemistry of this compound,[32,33] which has never been found to undergo cleavage in solution.

Experimentally, benzoyl and the benzil ketyl can also be distinguished in the following way. The main ketyl absorption moves from about 350 to 370 nm with decreasing acetonitrile to propan-2-ol content of the solution, while the ratio of absorbances of the short to the long wavelength maxima changes from 2 to 4. Further, addition of base to the solutions causes the appearance of the radical anion PhCOĊO$^-$Ph which has a strong red-shifted absorption.[14,15] Benzoyl does not show such behaviour, and we used the method of base addition to make sure that the benzil ketyl radical did not contribute to the spectra of Figure 5 and to those given below.

Figure 7 shows the spectrum of a radical obtained by photolysis of di(t-butyl) peroxide (2% by vol.) in acetonitrile containing 10% ω,ω-dimethoxytoluene (the dimethylketal of benzaldehyde) using a threefold larger intensity than in the other cases (Ni/Co filter solution). As evident from ESR observations (see below) under these conditions the dimethoxybenzyl radical is formed together with minor amounts of $^{\bullet}CH_2CN$ and $^{\bullet}CH_3$. Since only the benzyl-type radical is expected to absorb above 300 nm we attribute the spectrum to it. It agrees fully with the features known for other benzyl type radicals, *i.e.* strong transitions in the 300–320 nm region and weaker broad absorptions from 350–500 nm.[14,15,21,34,35] It should be noted that the absorbance of the dimethoxybenzyl radical in Figure 7

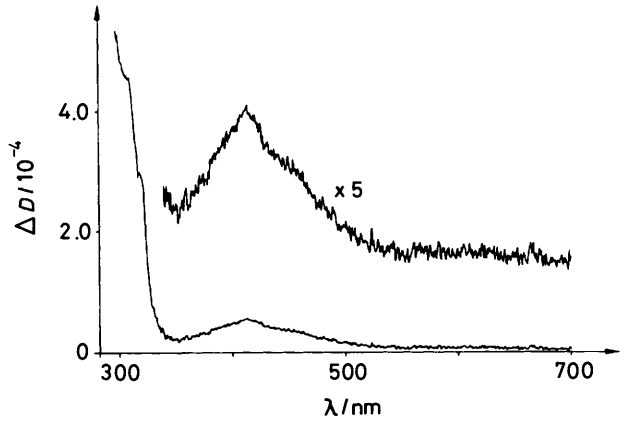

Figure 8. Optical spectrum ($\nu = 77\ s^{-1}$, $T = 27\ °C$) of $PhC(OCH_3)_2$ derived from DMPA in acetonitrile.

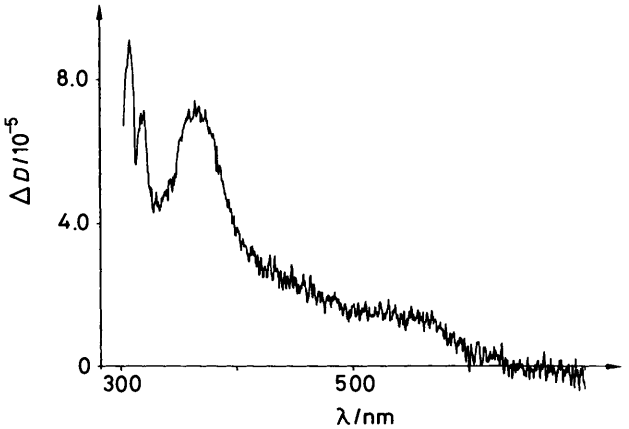

Figure 9. Optical spectrum ($\nu = 77\ s^{-1}$, $T = 21\ °C$) of transients from DMPA under high intensity photolysis.

exceeds considerably that of the benzoyl radicals (Figure 5), which points to a larger absorption coefficient.

In Figure 8 a radical spectrum from the photolysis of DMPA is displayed. It was obtained with the 365 nm radiation reduced to one-third the intensity used for the spectra of Figure 5. Comparison with Figure 7 shows exact agreement, *i.e.* the dimethoxybenzyl radical is observed. The formation of the benzoyl radical is not evident, which again points to a lower absorption.

It must be stressed that during DMPA photolysis a clear spectrum of dimethoxybenzyl could only be obtained for very low light intensities. Figure 9 gives a spectrum recorded with a twelvefold higher intensity than Figure 8. Now, the transitions of the benzyl-type radical are weakened and the typical 370 nm transition of benzoyl appears. Moreover, the total absorbance near 300 nm is considerably reduced despite the larger photolysis rate. This is direct proof of the photofragmentation.

As evident from the reported short radical lifetimes and their description of experimental details, the previous spectroscopic study of Fouassier *et al.*[3,6] on DMPA photoreactions used much larger light intensities, especially of the analysing beam (boosted 150 W lamp). As mentioned before, the spectral properties, shown for $\lambda \geq 390$ nm only, are not compatible with those of dimethoxybenzyl (the maximum at 418 nm was not observed) and vaguely resemble those of benzoyl or the benzil ketyl radical PhCOĊOHPh observed here. Quite obviously, the spectra and the kinetics of the previous work were highly influenced by photofragmentation and secondary photoreactions. The conclusions concerning the photochemical behaviour of DMPA derived from them are therefore also not now tenable.

Kinetic spectroscopy. Variation of the modulation frequency of photolysis of DMPA and phase-sensitive analysis of the radical signals as before[13,21,34,36] allows the determination of radical reaction rate constants and molar absorption coefficients. Such experiments were performed under conditions of negligible photofragmentation, *i.e.* for the spectrum of Figure 7, for two initial DMPA concentrations in acetonitrile (1.0 and 2.2×10^{-3} mol dm^{-3}) and at four wavelengths (304, 318, 450, and 500 nm). The low contribution of benzoyl to the spectra was neglected. The essential reactions of Scheme 2 can be condensed into the following equations,

$$\text{DMPA} \longrightarrow \mathbf{R}^1 + \mathbf{R}^2 \qquad \text{rate } I = \frac{I_0}{2}(1 + \cos \omega t)$$

$$\mathbf{R}^1 \longrightarrow (3) + \mathbf{R}^3 \qquad \text{rate constant } k_3$$

$$R^i + \mathbf{R}^j \longrightarrow \mathbf{P}^{ij} \qquad \text{rate constant } k_{ij}$$

where ω is the angular frequency of modulation, and k_{ij} denotes the termination constant for the reaction between radicals $\mathbf{R}^i$ and $\mathbf{R}^j$. To simplify the analysis we assume that all cross-termination rate constants k_{ij} ($i \neq j$) are equal, that the same holds for the self-terminations $2k_{ii}$, and that $k_{ij} = 2k_{ii} = 2k_t$. In fact, it is known that methyl and benzoyl radicals self-termination is diffusion-controlled, and the same holds for the more stabilized benzyl radical.[13,21,34,37,38] For the dimethoxybenzyl radical this reaction has not yet been observed, however the similarly sterically hindered α,α-dimethylbenzyl radical has $2k_t = 1.4 \times 10^9$ dm^3 mol^{-1} s^{-1} at room temperature in cyclohexane solvent,[35] *i.e.* also a nearly diffusion-controlled rate. The diffusion coefficients of the radicals $\mathbf{R}^1$, $\mathbf{R}^2$, and $\mathbf{R}^3$ were estimated to differ by not more than a factor of two, *i.e.* the following results cannot differ from the true values by more than this factor. Moreover, the product distribution (Table 1) gives no indication of slow terminations of $\mathbf{R}^1$.

With these assumptions the relevant kinetic equations are (18) and (19), where [R] is the total radical concentration. For

$$[\mathbf{R}^1] = I - \{k_3 + 2k_t[\mathbf{R}]\}[\mathbf{R}^1] \qquad (18)$$

$$[\mathbf{R}] = 2I - 2k_t[\mathbf{R}]^2 \qquad (19)$$

high enough modulation frequencies the concentrations are sums of larger time-independent and smaller oscillating terms, $[\mathbf{R}^i] = [\mathbf{R}^i]_0 + [\mathbf{R}^i]_{osc} \cos(\omega t + \varphi_i)$ of which the oscillating terms are detected as oscillating absorbances $\Delta D = \Sigma \varepsilon_i l [\mathbf{R}^i]_{osc}$, where l is the cell length.[21,36] Insertion of $[\mathbf{R}^i]$ into the kinetic equations leads with the usual linearization to equation (20) for

$$\Delta D^2 = \left(\frac{\varepsilon I_0 l \tau}{2}\right)^2 \times (1 + \omega^2\tau^2)^{-1} \qquad (20)$$

the absorbance of $\mathbf{R}^1$, where τ is an effective lifetime of $\mathbf{R}^1$,

$$\tau = \frac{\tau_1}{\left\{1 + \frac{\tau_1^3}{\tau_t^3}\left(4 - \frac{\tau_1}{\tau_t}\right)\right\}^{\frac{1}{3}}} \qquad (21)$$

composed of the overall termination lifetime $\tau_t = \{2k_t[\mathbf{R}]_0\}^{-1} = (2k_t I_0)^{-\frac{1}{2}}$ and

$$\tau_1 = \tau_t(1 + k_3\tau_t)^{-1} \qquad (22)$$

The expression for ΔD^2 shows that a plot of ΔD^{-2} *vs.* ω^2 should give a straight line from which τ and εI_0 can be determined. Figure 10 shows such a plot. It leads to $\tau = 1.4 \times 10^{-3}$ s and $\varepsilon I_0 = 0.15\ cm^{-1}\ s^{-1}$ at 318 nm. I_0 was obtained

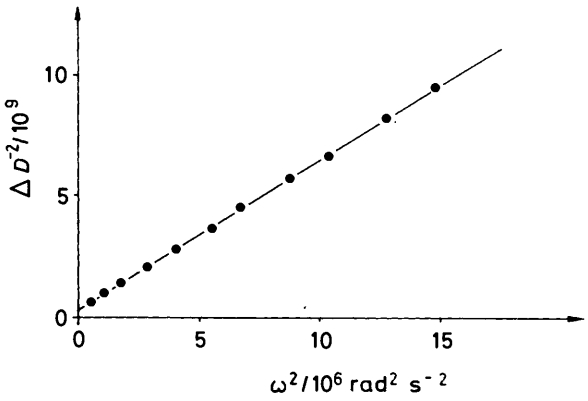

Figure 10. ΔD^{-2} *vs.* ω^2 for $PhC(OCH_3)_2$; τ = 1.41 ms, λ = 318 nm, T = 25 °C.

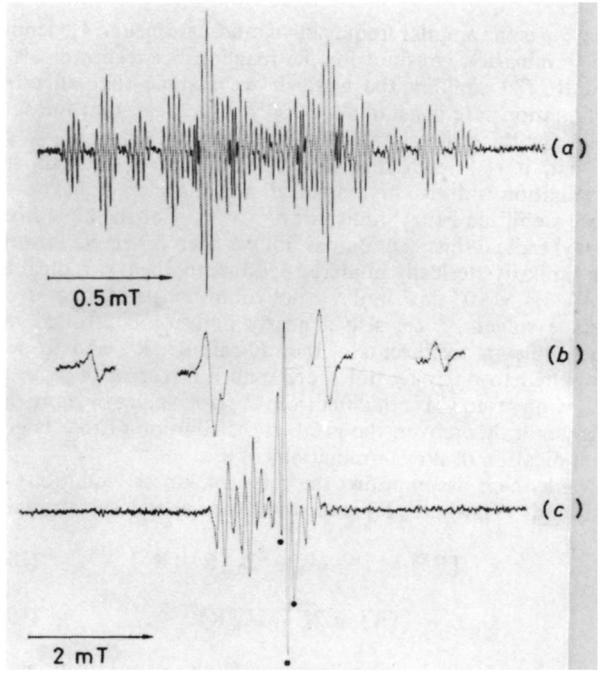

Figure 11. ESR spectra of radicals during photolysis of DMPA: (*a*) dimethoxybenzyl; (*b*) methyl at 71 °C; (*c*) benzoyl (●) and dimethoxybenzyl.

from the DMPA lifetime under modulated photolysis in stationary solutions,[21] and was found to be about 3 × 10^{-5} mol dm^{-3} s^{-1}.

For the conditions of the modulation experiments P_{DEM} is approximately given by equation (23), and it is known to be 0.55

$$P_{DEM} = k_3\tau_t(1 + k_3\tau_t)^{-1} \quad (23)$$

from the product analysis (Table 1). Thus, $2k_t$ and k_3 can be extracted from P_{DEM}, τ and I_0. The value of k_3, averaged from 21 individual determinations, is found * to be (260 ± 50)s^{-1} *i.e.* the value for the rate constant of thermal demethylation at room

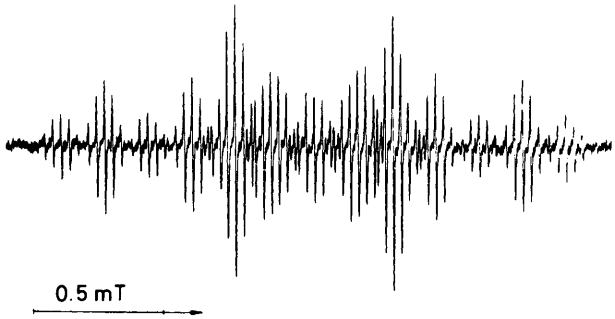

Figure 12. ESR spectrum of dimethoxybenzyl.

temperature. As assumed in the earlier sections this process is fairly slow. If a normal frequency factor is applied [log(A/s) = 13.3] the activation energy becomes E_a = 67.5 kJ mol^{-1}. This is not unreasonable if compared with E_a = 33 kJ mol^{-1} for the related fission[39] of $PhC(CH_3)_2O\dot{C}HCH_3$, since the latter yields the stabilized cumyl radical and since fragmentation rates depend on bond strengths.[40]

Table 5 lists the termination constant $2k_t$ and the decadic absorption coefficients of the radicals. Since acetonitrile is less viscous than 3-methylpentan-3-ol, $2k_t$ of $\mathbf{R}^2$ is larger in the former solvent. From the order of magnitude $2k_t$ is close to diffusion control. The absorption coefficients of $\mathbf{R}^1$, determined from the kinetic experiments, agree well with the spectra of Figures 6 and 7. Further, they are in agreement with the expectation for benzyl-type radicals and confirm the assumption of low spectral contributions of benzoyl for $\lambda \geq 320$ nm. Finally, they support a considerable photofragmentation during our laser pulse experiments. Under the conditions of the CIDNP observations 5.4 × 10^{-4} mol dm^{-3} radicals $\mathbf{R}^1$ are produced for 117 mJ pulses delivered to the probehead at 308 nm. They produce an absorbance of 1.04 at 308 nm, while the absorbance of DMPA was 0.87. Consequently, a considerable fraction of the light is absorbed by the radicals. From P_{DEM} *ca.* 0.25 we conclude that the quantum yield of the photofragmentation must be around 0.5.

Electron Spin Resonance.—CW–ESR spectroscopy with continuous photolysis was applied to study the radicals generated from DMPA and related systems and their addition to alkenes directly. As a model alkene acrylonitrile was used because most radicals add easily to this compound whereas the following propagation steps are rather slow. Acetonitrile and 3-methylpentan-3-ol were employed as solvents leading to identical results.

Figure 11(*a*) shows an ESR spectrum obtained during photolysis of 0.05 mol dm^{-3} DMPA in 3-methylpentan-3-ol with 1 mW microwave power. The signal is assigned to the dimethoxybenzyl radical. The completely emissive character is due to the occurrence of strong triplet CIDEP during the α-cleavage.[10,17] The benzoyl radical has broader lines. Figure 11(*c*) was taken with 5 mW microwave power, higher modulation amplitude and scan range and demonstrates the presence of benzoyl together with the now broadened features of dimethoxybenzyl. Methyl radicals were not detected at room temperature, *i.e.* there is little photofragmentation. The insert in Figure 11(*b*) shows part of the spectrum recorded at 71 °C with the lines of $^{\cdot}CH_3$ now formed by thermal fragmentation. Hageman *et al.*[8] observed only benzoyl and methyl by ESR during DMPA photolysis. If dimethoxybenzyl had not escaped their attention this suggests a much higher light intensity in their study and complete photofragmentation. The assignment of the spectrum shown in Figure 11(*a*) is supported by Figure 12. This spectrum was obtained by photolysis of 0.14 mol dm^{-3} di(t-butyl)peroxide in acetonitrile containing 0.27 mol dm^{-3} of the acetal $PhCH(OCH_3)_2$. The dimethoxybenzyl radical is formed

* *Note Added in proof.*—While the manuscript was in press we noted that reformation of DMPA by combination of $\mathbf{R}^1$ and $\mathbf{R}^2$ (1) had not been included in the analysis of dimethylation, though it can be taken into account *via* the CIDNP data presented. Reanalysis changed the values of kinetic constants to k_3 = (295 ± 50) s^{-1} and $2k_t$ = (3.2 ± 0.8) × 10^9 dm^3 mol^{-1} s^{-1}, *i.e.* within the error limits given in the text.

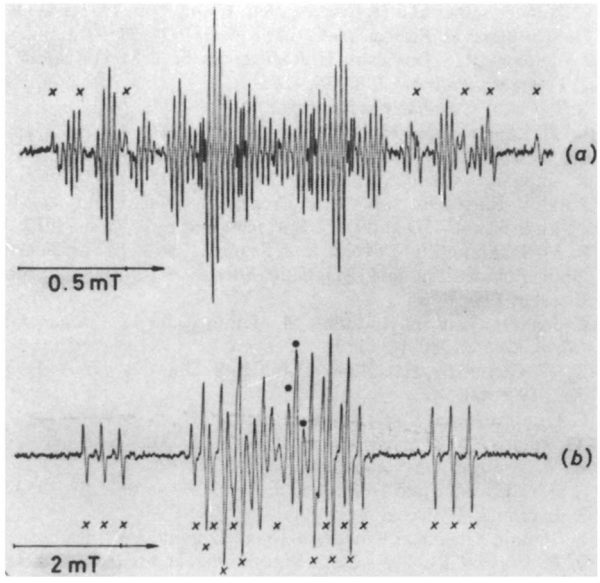

Figure 13. ESR spectra of radicals during photolysis of DMPA in acrylonitrile-containing solutions (0.025 mol dm^{-3}): (*a*) dimethoxybenzyl + $PhCOCH_2\dot{C}HCN$ (×); (*b*) benzoyl (●), $PhCOCH_2\dot{C}HCN$ (×). The remaining lines are due to dimethoxybenzyl.

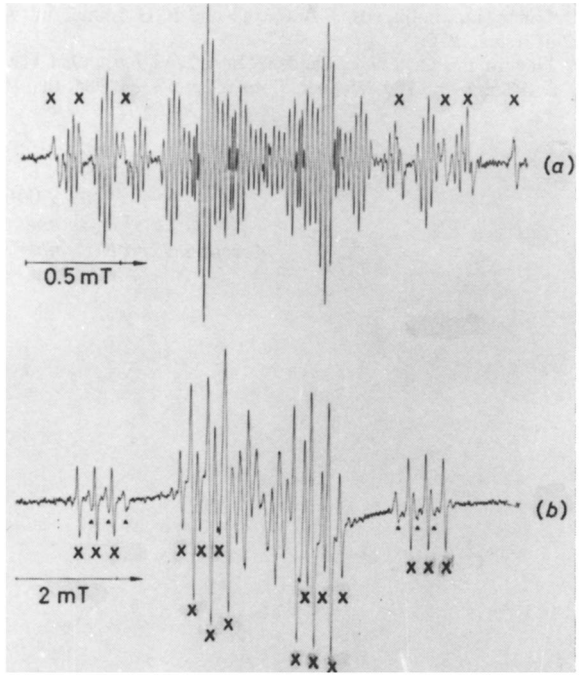

Figure 14. ESR spectra of radicals during photolysis of DMPA in acrylonitrile-containing solutions (0.15 mol dm^{-3}). Symbols as in Figure 13, but △ ≡ $PhCOCH_2CHCNCH_2\dot{C}HCN$.

by hydrogen abstraction and now shows normal absorption only. In the absence of the acetal $^{\bullet}CH_3$ and $^{\bullet}CH_2CN$ were also observed.

To obtain the spectrum of the adduct of benzoyl to acrylonitrile ESR spectra were taken during photolysis of solutions containing di(t-butyl)peroxide (0.14 mol dm^{-3}), benzaldehyde (0.2 mol dm^{-3}), and acrylonitrile (0–0.15 mol dm^{-3}). The benzoyl adduct was easily observed. With benzaldehyde-free solutions we also observed the adduct of $^{\bullet}CH_2CN$ (acetonitrile solvent) and $^{\bullet}CH_3$ (dominant in 3-methylpentan-3-ol). Corresponding experiments were carried out to observe the adduct of the dimethoxybenzyl radical with solutions containing peroxide, the acetal, and acrylonitrile, but these were unsuccessful. Signals of the adducts of $^{\bullet}CH_2CN$ and of benzoyl were found, the latter caused by a benzaldehyde impurity, but the desired adduct was not obtained. Obviously, dimethoxybenzyl radicals do not add easily to acrylonitrile. This is supported by the spectra shown in Figures 13 and 14, obtained under the conditions used for Figure 11 with DMPA solutions but in the presence of 0.025 and 0.15 mol dm^{-3} acrylonitrile, respectively. The signal of the dimethoxybenzyl radical is not quenched whereas benzoyl disappeared and is replaced by the adduct $Ph\dot{C}OCH_2CHCN$. For the higher concentration the dimer radical $PhCOCH_2CHCNCH_2\dot{C}HCN$ is also visible.

Table 6. ESR parameters of new adduct radicals.

Radical	Solvent,[a] *T*/K	*g*	*a*-Values/mT
$PhCOCH_2\text{-}\dot{C}HCN$	3-MP, 303	2.0031	H_α:2.05 $2H_\beta$:2.25 N:0.35
$NC\text{-}CH_2\text{-}\dot{C}H_2\text{-}CHCN$	ACN, 293	2.0030	H_α:2.05 $2H_\beta$:2.45 N:0.35
$PhCOCH_2CHCN\text{-}CH_2\text{-}\dot{C}HCN$	3-MP, 303	2.0031	H_α:1.90 $2H_\beta$:2.20 N:0.35

[a] 3-MP = 3-methylpentan-3-ol, ACN = acetonitrile.

From the acrylonitrile concentrations and an estimated termination life-time of about 1 ms for our ESR conditions, the rate constant for addition of the dimethoxybenzyl radical must be smaller than 10^4 dm^3 mol^{-1} s^{-1}, while that for benzoyl is in the 10^5 to 10^6 dm^3 mol^{-1} s^{-1} region and similar to that of $(CH_3)_3C\dot{C}O$.[29] These findings agree with the product analysis of Hageman *et al.*,[8] and support the conclusion that benzoyl and methyl effectively initiate photopolymerizations with DMPA, whereas dimethoxybenzyl does not. Of course, a minor contribution at very high monomer concentrations can not yet be ruled out from our upper limit of the addition rate constant.

So far, little is known on absolute rate constants for addition of benzyl radicals to alkenes. They are certainly lower than those of non-conjugated carbon radicals because the resonance stabilization is partly lost by the addition. This effect is well known from the copolymerization parameters of styryl radicals[41] but remains to be quantified. Table 6 lists the ESR data of radicals which were not yet reported in the literature.

Conclusions

A facile photofragmentation and a slow thermal fragmentation are probably common features of α-oxy-substituted benzyl radicals[18,39,42,43] and both affect the reaction mechanisms and kinetics of photoinitiators involving such species. In view of the present findings many previous seemingly contradictory reports on DMPA can easily be explained, *e.g.* the non-observation of methyl radicals by Timpe *et al.*[9] points to low intensity and rapid scavenging of the precursor, while Hageman,[8] Rist,[7] and Moebius[10] used fairly high intensity light. Fouassier's spectra and conclusions were even falsified by the photofragmentation.[6,12]

Photocuring with DMPA normally implies the use of high light intensities where the photofragmentation is important. The comparably high efficiency of this initiator may well be related to this process but without careful analysis of experiments performed under technical conditions this point remains open.

Acknowledgements

We thank the Swiss National Science Foundation for financial support, Ciba–Geigy for a generous gift of chemicals and deuteriated solvents and Drs. H. U. Dütsch and P. Burkhard for early contributions to this work.

References

1 R. Kirchmayr, G. Berner, and G. Rist, *Farbe + Lack*, 1980, **86**, 224, and references therein.
2 H. J. Hageman, *Prog. Org. Coat.*, 1985, **13**, 123, and references therein.
3 J. P. Fouassier, P. Jaques, D. J. Lougnot, and T. Pilot, *Polym. Photochem.*, 1984, **5**, 57, and references therein.
4 M. R. Sandner and C. L. Osborn, *Tetrahedron Lett.*, 1974, 415.
5 F. D. Lewis, R. T. Lauterbach, H.-G. Heine, W. Hartmann, and H. Rudolph, *J. Am. Chem. Soc.*, 1975, **97**, 1519.
6 J. P. Fouassier and A. Merlin, *J. Photochem.*, 1980, **12**, 17.
7 A. Borer, R. Kirchmayr, and G. Rist, *Helv. Chim. Acta*, 1978, **61**, 305.
8 C. J. Groenenboom, H. J. Hageman, T. Overeem, and A. J. M. Weber, *Makromol. Chem.*, 1982, **183**, 281.
9 H. Baumann, H. J. Timpe, V. E. Zubarev, N. V. Fok, and M. Y. Melnikov, *J. Photochem.*, 1985, **30**, 487.
10 P. Jaegermann, F. Lendzian, G. Rist, and K. Möbius, *Chem. Phys. Lett.*, 1987, **140**, 615.
11 H. R. Dütsch, Diploma Thesis, Zürich, 1975.
12 A. Merlin and J. P. Fouassier, *Makromol. Chem.*, 1980, **181**, 1307.
13 C. Huggenberger, J. Lipscher, and H. Fischer, *J. Phys. Chem.*, 1980, **84**, 3467.
14 A. Beckwith, A. D. Osborne, and G. Porter, *Trans. Faraday Soc.*, 1964, **60**, 873.
15 E. Hayon, T. Ibaya, N. N. Lichtin, and M. Simic, *J. Phys. Chem.*, 1972, **76**, 2072.
16 N. S. Allen, F. Catalina, P. N. Green, and W. A. Green, *Eur. Polym. J.*, 1986, **22**, 49.
17 F. Jent, H. Paul, and H. Fischer, *Chem. Phys. Lett.*, 1988, **146**, 315.
18 L. J. Johnston, D. J. Lougnot, and J. C. Scaiano, *Chem. Phys. Lett.*, 1986, **129**, 205.
19 J. K. Vollenweider, H. Fischer, J. Hennig, and R. Leuschner, *Chem. Phys.*, 1985, **97**, 217.
20 J. K. Vollenweider and H. Fischer, *Chem. Phys.*, 1988, **124**, 333.
21 C. Huggenberger and H. Fischer, *Helv. Chim. Acta*, 1981, **64**, 338.
22 H. Schuh and H. Fischer, *Helv. Chim. Acta*, 1978, **57**, 2011.
23 J. E. Baxter, R. S. Davidson, H. J. Hageman, G. T. M. Hakvoort, and T. Overeem, *Polymer*, 1988, **29**, 1575.
24 X. T. Phan, *J. Radiat. Curing*, 1986, 11.
25 (*a*) H. Langhals and H. Fischer, *Chem. Ber.*, 1978, **111**, 1978; (*b*) M. Läufer and H. Dreeskamp, *J. Magn. Reson.*, 1984, **60**, 357.
26 R. Kaptein, *J. Chem. Soc., Chem. Commun.*, 1971, 732.
27 Landolt–Börnstein, 'Magnetic Properties of Free Radicals,' ed. H. Fischer, vols II/9 and II/17, Springer, Berlin, 1980 and 1987.
28 K. M. Salikhov, Yu N. Molin, R. Z. Sagdeev, and A. L. Buchachenko, 'Spin Polarization and Magnetic Effects in Radical Reactions,' Elsevier, 1984.
29 F. Jent, H. Paul, E. Roduner, M. Heming, and H. Fischer, *Int. J. Chem. Kinet.*, 1986, **18**, 1113.
30 K. W. Chambers, E. Collinson, and F. S. Dainton, *Trans. Faraday Soc.*, 1970, **66**, 142.
31 C. Huggenberger, Ph.D. Thesis, Zürich, 1981.
32 M. Rubin, *Fortschr. Chem. Forsch.*, 1969, **13**, 251.
33 B. M. Monroe, *Adv. Photochem.*, 1971, **8**, 77.
34 R. F. C. Claridge and H. Fischer, *J. Phys. Chem.*, 1983, **87**, 1960.
35 R. Baer and H. Fischer, to be published.
36 H. Paul in 'Chemical Kinetics of Small Organic Alkyl Radicals,' ed. Z. B. Alfassi, CRC Press, Boca Raton, 1988, and references therein.
37 M. Lehni, H. Schuh, and H. Fischer, *Int. J. Chem. Kinet.*, 1979, **11**, 705.
38 Landolt–Börnstein, 'Radical Reaction Rates in Liquids,' vol. II/13a, ed. H. Fischer, Springer, 1984.
39 S. Steenken, H. P. Schuchmann, and C. von Sonntag, *J. Phys. Chem.*, 1975, **79**, 763.
40 H. Fischer and H. Paul, *Acc. Chem. Res.*, 1987, **20**, 200.
41 Polymer Handbook, eds. J. Brandrup and E. H. Immergut, Wiley, Chichester, 1975.
42 V. Nagarajan and R. W. Fessenden, *Chem. Phys. Lett.*, 1984, **112**, 207.
43 J. C. Scaiano and P. J. Wagner, *J. Am. Chem. Soc.*, 1984, **106**, 4626.

Paper 9/04676C
Received 31*st October* 1989
Accepted 22*nd November* 1989